

Lifetime laser damage performance of β -Ga₂O₃ for high power applications

Jae-Hyuck Yoo, Subrina Rafique, Andrew Lange, Hongping Zhao, and Selim Elhadj

Citation: *APL Materials* **6**, 036105 (2018); doi: 10.1063/1.5021603

View online: <https://doi.org/10.1063/1.5021603>

View Table of Contents: <http://aip.scitation.org/toc/apm/6/3>

Published by the [American Institute of Physics](#)

Articles you may be interested in

[A review of Ga₂O₃ materials, processing, and devices](#)

Applied Physics Reviews **5**, 011301 (2018); 10.1063/1.5006941

[High breakdown voltage quasi-two-dimensional \$\beta\$ -Ga₂O₃ field-effect transistors with a boron nitride field plate](#)

Applied Physics Letters **112**, 122102 (2018); 10.1063/1.5018238

[Minimizing performance degradation induced by interfacial recombination in perovskite solar cells through tailoring of the transport layer electronic properties](#)

APL Materials **6**, 036104 (2018); 10.1063/1.5021138

[High breakdown electric field in \$\beta\$ -Ga₂O₃/graphene vertical barristor heterostructure](#)

Applied Physics Letters **112**, 032101 (2018); 10.1063/1.5002138

[Guest Editorial: The dawn of gallium oxide microelectronics](#)

Applied Physics Letters **112**, 060401 (2018); 10.1063/1.5017845

[Controlling n-type conductivity of \$\beta\$ -Ga₂O₃ by Nb doping](#)

Applied Physics Letters **111**, 242103 (2017); 10.1063/1.4994263



Running in circles looking
for the best **science job?**

Search hundreds of exciting
new jobs each month!

PHYSICS TODAY | JOBS
www.physicstoday.org/jobs

Lifetime laser damage performance of β -Ga₂O₃ for high power applications

Jae-Hyuck Yoo,¹ Subrina Rafique,^{2,3} Andrew Lange,¹ Hongping Zhao,^{2,3,4} and Selim Elhadj^{5,a}

¹Physical and Life Sciences and NIF and Photon Sciences, Lawrence Livermore National Laboratory, 7000 East Avenue, Livermore, California 94550, USA

²Department of Electrical and Computer Engineering, The Ohio State University, Columbus, Ohio 43210, USA

³Department of Electrical Engineering and Computer Science, Case Western Reserve University, Cleveland, Ohio 44106, USA

⁴Department of Materials Science and Engineering, The Ohio State University, Columbus, Ohio 43210, USA

⁵Materials Engineering Division and NIF and Photon Sciences, Lawrence Livermore National Laboratory, 7000 East Avenue, Livermore, California 94550, USA

(Received 5 January 2018; accepted 28 February 2018; published online 20 March 2018)

Gallium oxide (Ga₂O₃) is an emerging wide bandgap semiconductor with potential applications in power electronics and high power optical systems where gallium nitride and silicon carbide have already demonstrated unique advantages compared to gallium arsenide and silicon-based devices. Establishing the stability and breakdown conditions of these next-generation materials is critical to assessing their potential performance in devices subjected to large electric fields. Here, using systematic laser damage performance tests, we establish that β -Ga₂O₃ has the highest lifetime optical damage performance of any conductive material measured to date, above 10 J/cm² (1.4 GW/cm²). This has direct implications for its use as an active component in high power laser systems and may give insight into its utility for high-power switching applications. Both heteroepitaxial and bulk β -Ga₂O₃ samples were benchmarked against a heteroepitaxial gallium nitride sample, revealing an order of magnitude higher optical lifetime damage threshold for β -Ga₂O₃. Photoluminescence and Raman spectroscopy results suggest that the exceptional damage performance of β -Ga₂O₃ is due to lower absorptive defect concentrations and reduced epitaxial stress. © 2018 Author(s). All article content, except where otherwise noted, is licensed under a Creative Commons Attribution (CC BY) license (<http://creativecommons.org/licenses/by/4.0/>). <https://doi.org/10.1063/1.5021603>

Gallium oxide (Ga₂O₃) has recently gained attention for high-power switching applications due to its high Baliga figure of merit¹ and the ability to grow large-area single crystals from the melt. Its outstanding material properties can in principle enable power devices with higher operating voltages and efficiencies compared to competing materials.² In this study, we systematically consider the use of β -Ga₂O₃ for high power optoelectronic applications by using short, high-energy laser pulses to assess the material's lifetime damage performance at GW/cm² intensities, representative of fluences in high energy laser systems.^{3–5} Samples were illuminated with sub-bandgap energy (1.16 eV, 1064 nm) using a near infrared (NIR) laser with a 7 ns pulse length and 10 Hz repetition rate. Using exposures from a rep-rated pulsed laser^{6,7} is a practical means to assess the peak and average power lifetime damage threshold of β -Ga₂O₃ without the use of a device test setup to emulate repetitive field-switching conditions. Furthermore, the direct relationship between damage from the electric field of a laser beam and DC breakdown in wide bandgap materials^{8–11} suggests the possibility of using optical probing, as described here, to assess the relative lifetime performance of wide bandgap semiconductors used in power electronics (i.e., using light energy below the bandgap energy of the

^aAuthor to whom correspondence should be addressed: elhadj2@llnl.gov

material). Such AC electric fields at optical frequencies generated during pulse exposures can exceed the critical breakdown field, especially when defect states act as shallow donors to seed electrons for avalanche ionization and catastrophic absorption, or the laser exposures can even induce damage at lower electric fields by free electron absorption and thermal degradation. Likewise, DC breakdown can occur when fields exceed the intrinsic breakdown field of a material, determined at least in part by its bandgap, or at lower fields when defects reduce the breakdown voltage and lifetime performance.¹² In general, for laser exposures larger than 10 ps, heat diffusion and defect absorption play a dominant role in determining the damage threshold,¹³ while ultrashort pulses less than 10 ps can be used to probe intrinsic damage processes.^{14,15}

The optical strength and the extent of light energy coupling of an n-doped β -Ga₂O₃ film were thus assessed and benchmarked with that of a comparable n-doped gallium nitride (GaN) sample. Both films were grown heteroepitaxially on sapphire by chemical vapor deposition (CVD).^{16,17} The single crystal, bulk lifetime damage performance of n-doped β -Ga₂O₃ was also determined using a substrate grown by the floating zone (FZ) melt growth technique.¹⁸ Despite its comparatively lower thermal conductivity, β -Ga₂O₃ can be grown directly on sapphire without the use of a buffer layer due to better lattice matching compared to GaN.¹⁷ Unlike bulk GaN and SiC, β -Ga₂O₃ can be grown from the melt without the use of supercritical pressures,² thereby lowering the cost of synthesis and avoiding the formation of extended defects such as dislocations and micropipes which are commonly found in GaN and SiC heteroepitaxial structures.^{19,20} The ability to grow bulk β -Ga₂O₃ crystals also facilitates scale-up for large area semiconductor manufacturing and presents opportunities for making vertically integrated devices. Therefore, given its thermal stability (up to \sim 1400 °C), wide bandgap ($E_g = 4.85$ eV), and lower dislocation density of 10^3 - 10^4 cm⁻²,² we expect β -Ga₂O₃ to be an ideal system for optically robust transparent electrodes in the UV-NIR range and for photonic, plasmonic, or optical coatings in the mid to far infrared range.^{21,22} The results presented here on the laser damage performance of β -Ga₂O₃ are the first of their kind and should be helpful in guiding the development of wide bandgap semiconductor materials for high power optoelectronic applications where optical absorption, electrical conductivity, and photo-electric properties are key design parameters.

Lifetime laser damage measurements were carried out on a conductive, Sn-doped, single crystal β -Ga₂O₃ substrate,²³⁻²⁵ a Si-doped β -Ga₂O₃ film grown on c-plane sapphire,^{16,17} and a Si-doped GaN film grown on c-plane sapphire using a 20 nm, low temperature GaN seed layer (Kyma Tech.).²⁶ The same growth orientation of the β -Ga₂O₃ bulk and film samples was $[\bar{2}01]$, and the orientation of the GaN sample was $[001]$. The lifetime damage threshold energy (energy at which damage is initiated) was determined using a fixed number of repeated pulse exposures as the damage threshold can depend on the number of exposures due to fatigue or incubation phenomena.^{27,28} For semiconductor materials, threshold values tend to saturate to a minimum after \sim 100 pulses.⁶ Therefore, laser damage tests were carried out with up to 1000 pulses. Damage was determined using optical microscopy. Due to the limited surface area of the samples and time-consuming nature of lifetime measurements at a repetition rate of 10 Hz, the results presented are limited to small beam tests (90 μ m $1/e^2$ diameter \times 10 spots). These tests probe damage initiated within areas of high defect densities; isolated, sparse defects are not sampled. However, since the same beam size was used for all samples, results can be compared directly. More details of the laser damage system and procedures used can be found in a previous report.²⁸ The measured properties of the tested materials and the laser parameters used in this study are summarized in Table I.

Representative damage morphologies are shown in Fig. 1 for the Sn-doped bulk β -Ga₂O₃ sample [Fig. 1(a)], β -Ga₂O₃ film [Fig. 1(b)], and GaN film [Fig. 1(c)], revealing commonly observed ablation and eruption pits.⁷ Single-pulse irradiation ($N = 1$) of the β -Ga₂O₃ bulk at 59 J/cm² produced a round, bulk ablation site with a depth of \sim 100 nm as shown in Fig. 1(a). A round ablation site morphology was maintained after exposing the bulk β -Ga₂O₃ sample to 100 pulses ($N = 100$) with fluences of 19.5 J/cm² (well above the damage threshold), while the damage depth was roughly 5.7 μ m. This result suggests damage initiated at the surface and propagated downward into the bulk. In contrast, single pulse irradiation of the β -Ga₂O₃ film at 19.3 J/cm² (also well above its damage threshold) tended to produce irregular damage morphologies as shown in Fig. 1(b). This differs from hexagonally shaped pits typically seen in ablated GaN films [Fig. 1(c)]. These differences in damage morphologies are related to differences in crystallography and the presence of well-defined cleavage planes for GaN.⁷

TABLE I. Measured electro-optical properties and lifetime laser damage thresholds of β -Ga₂O₃ and GaN samples. For lifetime damage threshold measurements (F_{th}), a 7 ns, 1064 nm laser with a beam $1/e^2$ diameter of 90 μ m was used to apply a number, N , of repeated pulsed irradiations at normal incidence. The bulk β -Ga₂O₃, grown by a floating zone (FZ) melt growth technique, was n-doped with tin (Sn); the heteroepitaxial film of β -Ga₂O₃, grown on sapphire (Al₂O₃) by low pressure chemical vapor deposition (LPCVD), was n-doped with silicon (Si); and the heteroepitaxial film of GaN, grown on sapphire by metal organic CVD (MOCVD), was n-doped with Si.

Samples	Substrate	Growth method	Thickness (μ m)	Sheet resistance (Ω/\square)	Mobility (cm^2/Vs)	Carrier concentration ($\times 10^{18}/\text{cm}^3$)	T at 1064 nm (%)	F_{th} ($N = 1$) (J/cm^2)	F_{th} ($N = 10$) (J/cm^2)	F_{th} ($N = 100$) (J/cm^2)	F_{th} ($N = 1000$) (J/cm^2)
($\bar{2}01$) β -Ga ₂ O ₃ bulk	...	FZ (Tamura, Inc.)	680	0.685	71.9	1.863	70.4	54.0 ($\pm 2\%$)	40.7 ($\pm 3\%$)	12.9 ($\pm 4\%$)	11.0 ($\pm 8\%$)
($\bar{2}01$) β -Ga ₂ O ₃ film	Al ₂ O ₃	LPCVD ¹⁶	12.5	36.5	72.1	1.897	67.0	14.3 ($\pm 1\%$)	9.1 ($\pm 1\%$)	9.6 ($\pm 5\%$)	7.7 ($\pm 10\%$)
(001) GaN film	Al ₂ O ₃	MOCVD (Kyma Tech.)	3.6	48.3	225	1.596	73.5	3.2 ($\pm 4\%$)	2.0 ($\pm 3\%$)	1.4 ($\pm 11\%$)	1.3 ($\pm 13\%$)

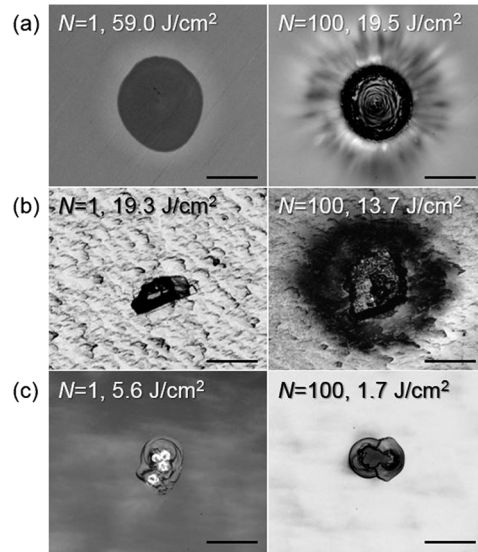


FIG. 1. Laser confocal micrographs of laser-induced damage in (a) β -Ga₂O₃ bulk, (b) LPCVD β -Ga₂O₃ film, and (c) MOCVD GaN film. Number of pulses (N) and laser fluences (F) are indicated. The scale bar in all images represents 50 μm . A 7 ns, 1064 nm laser with a beam $1/e^2$ diameter of 90 μm was used for the damage tests.

The damage area in the β -Ga₂O₃ film increased with repeated exposures for all samples tested. As shown in the *in situ* video S1 of the [supplementary material](#), damage associated with plasma emissions appeared to initiate below the β -Ga₂O₃ film surface which was followed by an abrupt eruption of material and plasma illumination from the damage site. This observation suggests, as was the case of GaN on sapphire,⁷ that absorption and damage initiates at the interface between the β -Ga₂O₃ film and sapphire substrate. For the GaN film shown in Fig. 1(c), eruptions and pit formation were observed in discrete locations related to local defect-driven absorption processes as reported previously.^{6,7}

In order to systemically determine laser damage thresholds with repeated exposures, we conducted multi-pulse laser damage tests over a range of fluences ($F = 1\text{--}100 \text{ J/cm}^2$ corresponding to intensities of 0.1–14.3 GW/cm²) and pulse numbers ($N = 1, 10, 100$, and 1000). Results from damage probability tests for $N = 1, 10, 100$, and 1000 pulses are summarized in the damage threshold fluence curves in Fig. 2. The dashed lines are based on an empirical fatigue model, $F_{th}(N) = F_{th}(\infty) + [F_{th}(1) - F_{th}(\infty)] \exp[-k(N - 1)]$, where k is an incubation factor and $F_{th}(N)$ is the damage threshold for

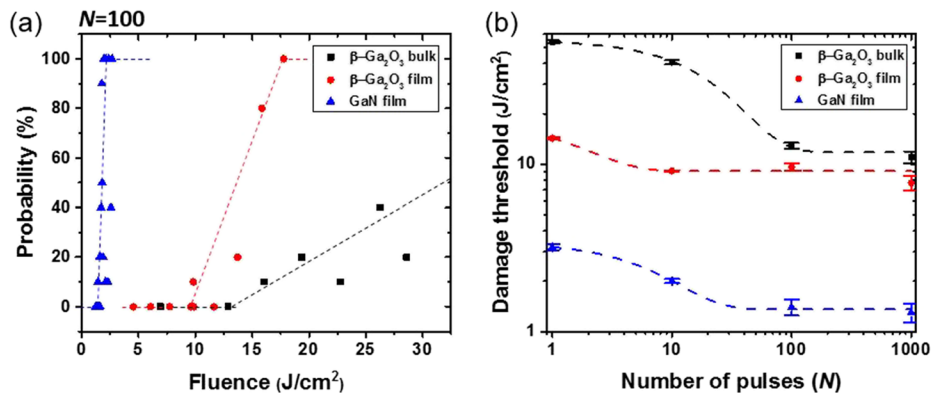


FIG. 2. (a) Representative damage curves for $N = 100$. The dashed lines are guide to the eye. (b) Comparison of the damage threshold fluences as a function of number of pulse exposures on a log-log scale for the GaN and β -Ga₂O₃ materials indicated. The lines are fit of the data based on a laser damage lifetime threshold fatigue model described in the text.

a given number of pulse exposures, N .²⁷ The stochastic nature of laser damage for the materials tested here was accounted for by using probability damage test curves [see examples in Fig. 2(a) for $N = 100$]; the damage sites appeared to be randomly distributed, likely due to NIR absorption near defects or clusters of defects formed during growth.⁶ The role of free electrons in absorption in the doped materials considered here is expected to be minimal because carrier densities were on the order of 10^{18} cm^{-3} .⁷ In semiconductor films with much larger carrier densities ($>10^{19} \text{ cm}^{-3}$),^{7,29} free carriers are the dominant source of absorption and damage becomes far more deterministic.

Each datum in the probability curves was obtained by dividing the total number of sites that appeared to damage at the specified fluence by the total number of sites tested (e.g., if 2 sites out of 10 are damaged, the probability was recorded as 20%). For single pulse exposures ($N = 1$), no damage was observed up to threshold (or damage onset) values of 54.0 J/cm^2 , 14.3 J/cm^2 , and 3.2 J/cm^2 for the $\beta\text{-Ga}_2\text{O}_3$ bulk sample, $\beta\text{-Ga}_2\text{O}_3$ film, and GaN film, respectively. However, for repeated exposures ($N > 1$), the threshold occurred at lower fluences compared to the single pulse thresholds, $F_{th}(N = 1)$, consistent with the increase in damage probability with increasing pulse number. The lifetime damage thresholds for $N = 1000$ occurred at fluences of 15 J/cm^2 , 10 J/cm^2 , and 1.5 J/cm^2 for the $\beta\text{-Ga}_2\text{O}_3$ bulk sample, the $\beta\text{-Ga}_2\text{O}_3$ film, and the GaN film, respectively. A summary of the damage threshold results for $N = 1, 10, 100$, and 1000 is shown in Table I. As expected, the damage thresholds stabilize as the number of pulse exposures increases, where the ratio $F_{th}(N = 1)/F_{th}(N = 1000)$ remains constant when $N > \sim 100$ down to between 30% and 70% of the $F_{th}(N = 1)$ value for all samples tested. The single pulse laser damage threshold of the bulk $\beta\text{-Ga}_2\text{O}_3$ sample was extremely high, roughly an order of magnitude higher than the other samples, and near the intrinsic damage threshold of high purity, occlusion free silica used in high power optics.²⁹ However, the lifetime threshold ($N = 1000$) of the bulk $\beta\text{-Ga}_2\text{O}_3$ sample was close, albeit slightly higher, to that of the $\beta\text{-Ga}_2\text{O}_3$ film indicating that optically induced “fatigue” mechanisms responsible for lowering the damage threshold are the same for both heteroepitaxial films and bulk materials. In comparison with the lifetime performance of the MOCVD GaN, the LPCVD $\beta\text{-Ga}_2\text{O}_3$ materials are proved to be much more robust by a factor of $\sim 10\times$. The $\beta\text{-Ga}_2\text{O}_3$ film considered here was also significantly more robust than high quality GaN produced by hydride vapor phase epitaxy (HVPE) ($\sim 2\times$) reported previously.⁶ Furthermore, the measured lifetime damage performances of both bulk and heteroepitaxial $\beta\text{-Ga}_2\text{O}_3$ are the highest demonstrated for any wide bandgap transparent conductive material, making $\beta\text{-Ga}_2\text{O}_3$ an ideal choice as a conductive material in optical systems when high power performance is critical.

We explored possible reasons for the superior lifetime damage performance of $\beta\text{-Ga}_2\text{O}_3$ by comparing the Raman spectrum and photoluminescence (PL) of the pristine, as-received samples. Raman spectra provide information about residual stresses due to the growth process, and PL spectra provide a means to qualitatively assess the concentration of optically absorbing defects present in these materials.

Confocal Raman spectroscopy with an excitation wavelength of 532 nm was performed at room temperature to probe all three samples [Figs. 3(a)–3(c)]. The Raman active modes detected for $\beta\text{-Ga}_2\text{O}_3$ include those associated with the liberation and translation of Ga_1O_4 chains ($<250 \text{ cm}^{-1}$), the deformation of Ga_1O_4 and Ga_2O_6 ($300\text{--}500 \text{ cm}^{-1}$), and the stretching and bending of Ga_1O_4 ($>600 \text{ cm}^{-1}$). These modes were detected for both the $\beta\text{-Ga}_2\text{O}_3$ bulk sample and the $\beta\text{-Ga}_2\text{O}_3$ film as shown in Figs. 3(a) and 3(b), respectively.^{30,31} The difference in relative peak intensities between the bulk sample and film may be attributed to the local strain induced by different dopants (Sn for the bulk sample vs Si for the film).²³ The peak centers of these Raman modes were almost identical for the two samples. However, a slight blue-shift ($<0.5 \text{ cm}^{-1}$) of the peaks was detected for the film relative to the bulk sample, suggesting a slight compressive stress in the film (assuming the bulk sample was stress free).^{32,33} The in-plane mismatch between the oxygen sublattice in $(\bar{2}01)$ $\beta\text{-Ga}_2\text{O}_3$ and the oxygen sublattice in c-plane sapphire is just 6.6%, half the lattice mismatch of GaN on sapphire (16.1%).³⁴ Therefore, $\beta\text{-Ga}_2\text{O}_3$ films are expected to have fewer dislocations resulting from stress relaxation.³⁵ In contrast, the Raman spectra of the GaN film in Fig. 3(c) have blue-shifted peaks such as E_g (575 cm^{-1}) and E_1 (748 cm^{-1}) modes with respect to the unstrained modes at 567 and 741 cm^{-1} , respectively.³⁶ Based on this blue-shift of $\sim 7.5 \text{ cm}^{-1}$, the GaN film was estimated to be under a high compressive stress of 2.2 GPa.^{3,37} This stress is due to both thermal expansion and lattice

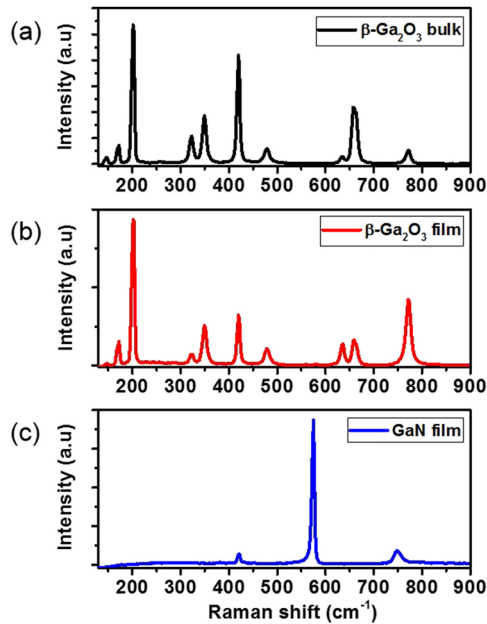


FIG. 3. Raman spectra of pristine, as-received samples of (a) β -Ga₂O₃ bulk, (b) LPCVD β -Ga₂O₃ film, and (c) MOCVD GaN film.

mismatch between the film and substrate. GaN and β -Ga₂O₃ materials have comparable thermal and mechanical stabilities and should, in principle, be able to tolerate similar levels of laser-induced heating and thermomechanical stress. Consequently, lower film stresses in β -Ga₂O₃ films grown on sapphire along with lower expected densities of strain related defects could account for the superior damage performance of β -Ga₂O₃ over GaN.

To probe the presence of potentially laser light absorbing defects, room temperature PL spectra were measured using a 280 nm (4.42 eV) excitation source (Fig. 4). Ultraviolet emissions around 400 nm were observed from the β -Ga₂O₃ bulk sample. The corresponding emission energy of 3.1 eV was previously found to be associated with the decay of excitons consisting of conduction band electrons bound to self-trapped holes.^{16,38} The emission was broader, and the peak intensity was 34% greater for the β -Ga₂O₃ film compared to the bulk β -Ga₂O₃ sample. This suggests that the film had more sub-bandgap defects as expected from being grown heteroepitaxially on sapphire. The GaN film showed near band edge emission (NBE) with a peak at 360 nm (3.44 eV) and broad

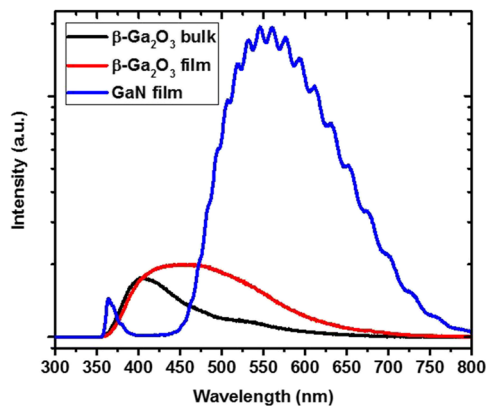


FIG. 4. Room temperature photoluminescence (PL) spectra of pristine, as-received samples of β -Ga₂O₃ bulk (black), LPCVD β -Ga₂O₃ film (red), and MOCVD GaN film (blue). All curves of PL intensity are shown on the same semi-log scale.

yellow luminescence (YL) near 550 nm (2.25 eV) which was previously associated with C_N-O_N complexes or substitutional C_N .^{7,39,40} The greater YL relative to the NBE peak also suggests lower crystal quality and the presence of a larger number of optically active defects in GaN compared to β -Ga₂O₃. Still, further studies are needed to probe the origins for the exceptional lifetime laser damage performance of β -Ga₂O₃ (2.1 GW/cm²) and to determine its utility for high performance, high power optoelectronics applications.

Heteroepitaxial and bulk β -Ga₂O₃ samples were benchmarked against a heteroepitaxial GaN sample revealing an order of magnitude higher optical lifetime damage threshold for β -Ga₂O₃. Photoluminescence and Raman spectroscopy suggest that the higher damage performance may be due to lower defect densities in bulk β -Ga₂O₃ and lower stresses in both bulk and heteroepitaxial β -Ga₂O₃. The lifetime laser damage threshold reported here for β -Ga₂O₃ is the highest of any conductive material to date, above 10 J/cm² (1.4 GW/cm²) demonstrating the potential of β -Ga₂O₃ for future high-power optoelectronics and electronics.

See [supplementary material](#) for a real-time video of a laser irradiated 12.5 μ m thick β -Ga₂O₃ film sample on sapphire using an above-damage threshold fluence (14 J/cm², 10 Hz, normal incidence) captured at an angle. Each pulse results in laser light energy absorption and damage-related plasma emissions emanating from below the film surface, followed by an abrupt eruption of material and direct exposure to intense plasma light emissions. This video confirms that laser damage initiates below the surface, likely beginning at the sapphire/ β -Ga₂O₃ interface where lattice mismatch strain dislocations are concentrated.

This work was performed under the auspices of the U.S. Department of Energy by Lawrence Livermore National Laboratory under Contract No. DE-AC52-07NA27344 within the LDRD program. Project No. 15-ERD-057 was funded by the LDRD Program at LLNL. Rafique and Zhao acknowledge the funding support from the National Science Foundation (No. DMR-1755479).

- ¹ B. J. Baliga, *J. Appl. Phys.* **53**(3), 1759 (1982).
- ² M. Higashiwaki, K. Sasaki, H. Murakami, Y. Kumagai, A. Koukitu, A. Kuramata, T. Masui, and S. Yamakoshi, *Semicond. Sci. Technol.* **31**(3), 034001 (2016).
- ³ I. Ahmad, M. Holtz, N. N. Faleev, and H. Temkin, *J. Appl. Phys.* **95**(4), 1692 (2004).
- ⁴ A. A. S. Awwal, M. Bowers, J. Wisoff, M. Herrmann, T. Anklam, J. Dawson, J.-M. Di Nicola, C. Haefner, M. Hermann, D. Larson, C. Marshall, B. Van Wonerghem, and P. Wegner, *Proc. SPIE* **10084**, 1008403 (2017).
- ⁵ G. Korn, L. O. Silva, C. L. Haefner, A. Bayramian, S. Betts, R. Bopp, S. Buck, J. Cupal, M. Drouin, A. Erlandson, J. Horáček, J. Horner, J. Jarboe, K. Kasl, D. Kim, E. Koh, L. Koubíková, W. Maranville, C. Marshall, D. Mason, J. Menapace, P. Miller, P. Mazurek, A. Naylor, J. Novák, D. Peceli, P. Rosso, K. Schaffers, E. Sistrunk, D. Smith, T. Spinka, J. Stanley, R. Steele, C. Stolz, T. Suratwala, S. Telford, J. Thoma, D. VanBlarcom, J. Weiss, and P. Wegner, *Proc. SPIE* **10241**, 1024102 (2017).
- ⁶ S. Elhadj, J. H. Yoo, R. A. Negres, M. G. Menor, J. J. Adams, N. Shen, D. A. Cross, I. L. Bass, and J. D. Bude, *Opt. Mater. Express* **7**(1), 202 (2017).
- ⁷ J. H. Yoo, M. G. Menor, J. J. Adams, R. N. Raman, J. R. I. Lee, T. Y. Olson, N. Shen, J. Suh, S. G. Demos, J. Bude, and S. Elhadj, *Opt. Express* **24**(16), 17616 (2016).
- ⁸ E. Yablonovitch and N. Bloembergen, *Phys. Rev. Lett.* **29**(4), 907 (1972).
- ⁹ N. Bloembergen, *IEEE J. Quantum Electron.* **10**(3), 375 (1974).
- ¹⁰ D. Arnold and E. Cartier, *Phys. Rev. B* **46**(23), 15102 (1992).
- ¹¹ B. Kochman, K. Yeom, and J. Singh, *Appl. Phys. Lett.* **68**(14), 1936 (1996).
- ¹² J. L. Hudgins, G. S. Simin, E. Santi, and M. A. Khan, *IEEE Trans. Power Electron.* **18**(3), 907 (2003).
- ¹³ B. C. Stuart, M. D. Feit, S. Herman, A. M. Rubenchik, B. W. Shore, and M. D. Perry, *Phys. Rev. B* **53**(4), 1749 (1996).
- ¹⁴ C. J. Stolz, R. A. Negres, K. Kafka, E. Chowdhury, M. Kirchner, K. Shea, and M. Daly, *Proc. SPIE* **9632**, 96320C (2015).
- ¹⁵ R. A. Negres, C. J. Stolz, K. R. P. Kafka, E. A. Chowdhury, M. Kirchner, K. Shea, and M. Daly, *Proc. SPIE* **10014**, 100140E (2016).
- ¹⁶ S. Rafique, L. Han, A. T. Neal, S. Mou, M. J. Tadjer, R. H. French, and H. Zhao, *Appl. Phys. Lett.* **109**(13), 132103 (2016).
- ¹⁷ S. Rafique, L. Han, and H. P. Zhao, *Phys. Status Solidi A* **213**(4), 1002 (2016).
- ¹⁸ N. Ueda, H. Hosono, R. Waseda, and H. Kawazoe, *Appl. Phys. Lett.* **71**(7), 933 (1997).
- ¹⁹ F. R. Chien, X. J. Ning, S. Stemmer, P. Pirouz, M. D. Bremser, and R. F. Davis, *Appl. Phys. Lett.* **68**(19), 2678 (1996).
- ²⁰ F. La Via, M. Camarda, and A. La Magna, *Appl. Phys. Rev.* **1**(3), 031301 (2014).
- ²¹ K. Feng, W. Streyer, Y. Zhong, A. J. Hoffman, and D. Wasserman, *Opt. Express* **23**(24), A1418 (2015).
- ²² G. Shkerdin, S. Rabbaa, J. Stiens, and R. Vounckx, *J. Phys. D: Appl. Phys.* **45**(49), 495103 (2012).
- ²³ T. Onuma, S. Fujioka, T. Yamaguchi, Y. Itoh, M. Higashiwaki, K. Sasaki, T. Masui, and T. Honda, *J. Cryst. Growth* **401**, 330 (2014).
- ²⁴ T. Onuma, S. Saito, K. Sasaki, T. Masui, T. Yamaguchi, T. Honda, A. Kuramata, and M. Higashiwaki, *Jpn. J. Appl. Phys., Part 1* **55**(12), 1202B2 (2016).

- ²⁵ S. Watanabe, K. Koshi, Y. Yamaoka, K. Iizuka, M. Takizawa, and T. Masui, U.S. patent application US2017/0152610 A1 (1 June 2017); JP patent application JP5749839B1 (30 June 2014).
- ²⁶ S. Nakamura, *Jpn. J. Appl. Phys., Part 2* **30**(10A), L1705 (1991).
- ²⁷ A. Rosenfeld, M. Lorenz, R. Stoian, and D. Ashkenasi, *Appl. Phys. A: Mater. Sci. Process.* **69**, S373 (1999).
- ²⁸ J. H. Yoo, A. Lange, J. Bude, and S. Elhadj, *Opt. Mater. Express* **7**(3), 817 (2017).
- ²⁹ J.-H. Yoo, M. Matthews, P. Ramsey, A. Correa Barrios, A. Carter, A. Lange, J. Bude, and S. Elhadj, *Opt. Express* **25**(21), 25533 (2017).
- ³⁰ D. Dohy, G. Lucazeau, and A. Revcolevschi, *J. Solid State Chem.* **45**(2), 180 (1982).
- ³¹ C. Kranert, C. Sturm, R. Schmidt-Grund, and M. Grundmann, *Sci. Rep.* **6**, 35964 (2016).
- ³² D. Machon, P. F. McMillan, B. Xu, and J. Dong, *Phys. Rev. B* **73**(9), 094125 (2006).
- ³³ R. Rao, A. M. Rao, B. Xu, J. Dong, S. Sharma, and M. K. Sunkara, *J. Appl. Phys.* **98**(9), 094312 (2005).
- ³⁴ D. Zhu, D. J. Wallis, and C. J. Humphreys, *Rep. Prog. Phys.* **76**(10), 106501 (2013).
- ³⁵ S. Nakagomi and Y. Kokubun, *J. Cryst. Growth* **349**(1), 12 (2012).
- ³⁶ M. Kuball, *Surf. Interface Anal.* **31**(10), 987 (2001).
- ³⁷ T. Kozawa, T. Kachi, H. Kano, H. Nagase, N. Koide, and K. Manabe, *J. Appl. Phys.* **77**(9), 4389 (1995).
- ³⁸ J. B. Varley, A. Janotti, C. Franchini, and C. G. Van de Walle, *Phys. Rev. B* **85**(8), 081109(R) (2012).
- ³⁹ J. L. Lyons, A. Janotti, and C. G. Van de Walle, *Appl. Phys. Lett.* **97**(15), 152108 (2010).
- ⁴⁰ M. A. Reshchikov, D. O. Demchenko, A. Usikov, H. Helava, and Y. Makarov, *Phys. Rev. B* **90**(23), 235203 (2014).